Journal of Photochemistry and Photobiology A: Chemistry 216 (2010) 126–132

Contents lists available at ScienceDirect

Journal of Photochemistry and Photobiology A: Chemistry

journal homepage: www.elsevier.com/locate/jphotochem

A low-cost procedure for the preparation of mesoporous layers of TiO_2 efficient in the environmental clean-up

Jiří Rathouský[a,*], Vít Kalousek[a], Viktor Yarovyi[b], Michael Wark[b], Jaromír Jirkovský[a]

[a] J. Heyrovský Institute of Physical Chemistry of AS CR, v.v.i., Dolejškova 3, 182 23 Prague 8, Czech Republic
[b] Institut für Physikalische Chemie und Elektrochemie, Leibniz Universität Hannover, Callinstraße 3-3a, 30167 Hannover, Germany

ARTICLE INFO

Article history:
Available online 9 June 2010

Keywords:
TiO_2
Mesoporous layers
Spray-coating
Photocatalysis
Gas-phase photocatalytic reactor
Nitrogen oxides
Self-cleaning surfaces

ABSTRACT

We have developed a low-cost procedure for the deposition of mesoporous films of TiO_2, which is easy to use and applicable for objects of various shape and size. This technique is based on spraying a sol containing titanium alkoxide, HCl, a suitable block-copolymer serving as a structure directing agent, and a solvent. Both the viscosity of the sol and the spraying conditions were precisely adjusted in order to achieve uniform coverage of the surface. The thickness of the films can be readily controlled by varying the number of deposited layers, their porosity being homogeneous and their surface area and pore volume increasing practically linearly with the increasing number of deposited layers. The mesoporous films of TiO_2 are suitable photocatalysts for the oxidation of NO and the removal of liquid layers deposited on their surface. The effect of the flow rate of the gaseous mixture through the reactor on the photocatalytic conversion of NO was analyzed.

1. Introduction

At present we are faced with the consequences of the pollution of the atmosphere of municipal cities and the soiling of the external surfaces of building structures [1]. Another very important general issue in a vast range of technologies is the requirement to render the surface of a number of products self-cleaning or at least easy-to-clean. Such a distinguished property would substantially enhance the utility value of the products and would improve the cleanness of the environment and consequently the quality of life.

Nitrogen oxides present in a concentration range of hundreds of ppb in air are responsible for urban smog because of their photochemical reactions with hydrocarbons and ozone as shown, e.g., by the data obtained in Guangzhou, Jerusalem and Paris [2–4]. Furthermore, together with sulphur dioxide and sulphur trioxide, they are the major contributors to the very harmful acid rain. Photocatalytic oxidation is a possible technology for the purification of air, whose main advantage over other oxidation treatments results from the direct absorption of light, which allows degrading the pollutants at ambient temperature, pressure and humidity [5–7]. Additionally, waste streams of low concentration and low flow rate can be processed. Weak UV irradiation of less than 1 mW/cm^2 in power needed for the photocatalytic conversion is amply provided by the solar light. More over, no extra reactants such as NH_3 or O_3 are required.

Another major environmental issue is the soiling of the external surfaces of buildings and other constructions. The ultimate goal is to provide their surfaces with such a finish, which will render them easy-to-clean or even self-cleaning. One of the possibilities is to cover their surface with a photocatalytically active layer. Such a layer should be active enough to decompose oxidatively organic deposits to inorganic products (CO_2, H_2O, and mineral acids). Consequently, the dust particles will no more stick on the irradiated surface and can be easily washed off by rain water. Additionally, such finishes often exhibit photoinduced superhydrophilicity, which further improves their self-cleaning ability.

Due to their unique properties, the anatase crystalline films with developed 3D mesoporosity can be photocatalysts of choice for the environmental applications [8–11]. In recent years, a generalized sol–gel procedure for the preparation of large-pore mesoporous films of metal oxides has been developed, which is based on a mechanism that combines evaporation-induced self-assembly (EISA) of a block-copolymer with complexation of molecular inorganic species enabling to prepare mesoporous films with good mechanical, optical and transport properties [12–14].

Mesoporous films of TiO_2 are especially effective when the photodecomposition mechanism includes reactants or intermediates adsorbed on the surface. The amount of adsorbed substances is increased due to the large surface area that enhances their decomposition rates. Further the mesoporosity will ensure fast transport of O_2 and H_2O, which are viable for the photocatalytic degradation of deposits. This transport can be significantly hindered by compact layers of dirt.

* Corresponding author: Tel.: +420 266053945; fax: +420 286582307.
E-mail address: jiri.rathousky@jh-inst.cas.cz (J. Rathouský).

1010-6030/$ – see front matter © 2010 Elsevier B.V. All rights reserved.
doi:10.1016/j.jphotochem.2010.06.002

The films are usually deposited by dip- or spin-coating, these procedures, however, being often technologically inconvenient and rather costly if objects with irregular shape or large size have to be coated. Eleven years ago, Brinker et al. [13] developed a procedure for the aerosol-assisted self-assembly of mesoporous nanoparticles. In a recent review, Sanchez et al. [14] suggested that EISA is compatible with chemical solution deposition techniques such as dip, spin, meniscus, and spray coatings. They stated that less attention was given to the construction of mesoporous materials and periodically organized mesoporous thin films using spray-coating, plasma driven sol–gel deposition, electrodeposition, electrospraying, and electrospinning.

In the present communication we report a low-cost procedure, which is easy to use and applicable for objects of various shape and size. This technique is based on spraying on a support a sol containing titanium alkoxide, HCl, a suitable block-copolymer serving as a structure directing agent, and a solvent. The viscosity of the spraying sol can be precisely adjusted in order to achieve uniform coverage of the surface. This technique is very often more suitable for coating larger or irregularly shaped objects than dip- or spin-coating. The main limitation of the size of the coated objects is the space capacity of the furnace, which can however be often overcome by an ingenious design of the oven. The clean-up of the effluent gases is not a great problem, as they contain only a small concentration of carbon dioxide and water vapour. It is a major advantage of non-ionic polyalkylene oxide copolymers, containing only carbon, hydrogen and oxygen, that no toxic gases are produced due to their thermal decomposition. These layers are shown efficient in the photocatalytic oxidation of NO and photocatalytic decomposition of layers of a model fatty dirt, namely oleic acid.

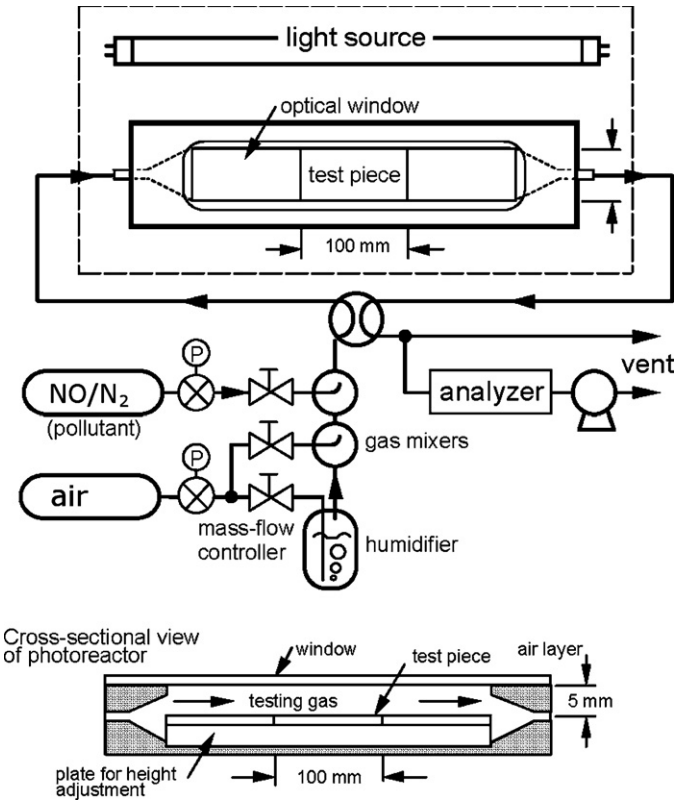

Fig. 1. Experimental set-up for the photocatalytic oxidation of gas streams containing a low concentration of NO at specified humidity.

2. Experimental

2.1. Preparation and characterization of the mesoporous films

The sol for the spraying was prepared by mixing 5 g of the ethylene oxide–propylene oxide block-co-polymer Pluronic P123, 56 mL of 1-butanol, 14.4 mL of titanium ethoxide and 10.2 mL of concentrated hydrochloric acid. For the spray-coating the sol was diluted with butanol in a ratio ranging from 1:100 to 1:5. The optimum diameter of the orifice in the spray-gun, air pressure and width of the sprayed area were 3 mm, 3 bar and 80–100 mm, respectively. The glass slides 50 mm × 100 mm in size, on which the sol was deposited, were preheated at 70 °C. After spraying, the layers were aged at room temperature with controlled humidity of 20% for 24 h and afterwards calcined at 350 °C for 3 h, this temperature being high enough to combust the Pluronic P123 copolymer to free the pores, yet low enough to avoid any destruction of the mesoporous structure. The FT-IR and Raman spectra of the films calcined at 350 °C did not show any traces of organic compounds. In order to obtain thicker films, the spraying procedure as well as the subsequent aging and calcination were repeated several times. All the chemicals were purchased from Sigma–Aldrich and were used without further purification.

The thickness of the films and the roughness of their surface were determined by a Dektak 150 profilometer. The crystallinity was assessed by the X-ray diffraction using a Siemens D 5005 diffractometer in the Bragg–Brentano geometry using CuKα radiation. The texture properties of the films were determined by the analysis of adsorption isotherms of Kr at 77 K measured with a Micromeritics ASAP 2010 volumetric adsorption unit using the method given in [15,16]. The details are provided in the Results section. The absorption spectra of mesoporous films were obtained with a Perkin-Elmer Lambda 19 spectrophotometer equipped with an integration sphere. First, transmitance (T) and reflectance (R) spectra of a glass slide with a thin film were measured. Then, the corresponding absorption spectrum (A) was calculated using the formula $A = 1 - T - R$. Finally, the absorbance spectrum (OD) was obtained employing the relation $OD = -\log(1 - A)$. The absorbance of a thin film at a particular wavelength was determined as a difference between the absorbance of a glass slide with and without a film. The surface morphology of thin films were examined by scanning electron microscope (SEM) using a Jeol JSM-6700F and also examined by transmission electron microscopy (TEM) using a Jeol JEM-2100 UHR microscope.

2.2. Photocatalysis

The experimental set-up for the photocatalytic tests in the gaseous phase consisted of a gas supply part, the photoreactor, and a chemiluminiscent Horiba ANPO 370 NO-NOx gas analyzer. The gaseous reaction mixture was prepared by mixing streams of dry air, wet air and NO/N_2, in order to obtain a final concentration of NO of 1 ppm at a relative humidity of 50%. The TiO_2 layers on glass slides were irradiated with three black light fluorescence lamps (Philips BLB 15 W, a length of 45 cm) in a planar arrangement, emitting dominantly at the wavelength of 365 nm. The distance between the lamps and the film was adjusted to achieve irradiation intensity of exactly 1 mW/cm^2 (Fig. 1). There is no change in the temperature due to the irradiation for the arrangements used.

The photocatalytic test itself was performed according to the following scheme. First the sample to be tested was cleaned by UV irradiation (2 mW/cm^2) for at least 5 h to decompose residual organic matter. The sample was inserted into the photoreactor, the distance between the sample and the window being adjusted. Afterwards the test gas was introduced into the photoreactor under dark conditions in order to equilibrate the adsorption of the gaseous NO/water vapour/air mixture on the surface of the

Table 1
The variation of the process parameters of the NO photocatalytic oxidation experiment.

Test	Linear velocity (cm s^{-1})	Dry air (mL s^{-1})	Wet air (mL s^{-1})	NO (mL s^{-1})	Sample–window distance (cm)
E1	10	10	10	0.47	0.4
E2	20	20	20	0.94	0.4
E3	10	25	25	1.17	1.0

Test	Theoretic photonic efficiency (%)	After switching on the light		After 120 min (steady state)	
		Photonic efficiency (%)	Relative photonic efficiency (%)	Photonic efficiency (%)	Relative photonic efficiency (%)
E1	0.12	0.12	98	0.10	79
E2	0.25	0.12	48	0.09	37
E3	0.32	0.15	49	0.12	39

photocatalyst. After achieving a constant gas concentration at the outlet, the irradiation was started and the concentration of NO and NO_2 was followed. An overview of experimental conditions is provided in Table 1, the test E3 corresponding to the ISO standard.

The self-cleaning performance of mesoporous TiO_2 films was tested by following the decomposition of a layer of oleic acid according to a slightly modified test method suggested as an ISO standard. Prior to the photocatalytic tests, the test pieces were purified by a UV light irradiation (2 mW/cm^2) for 24 h. Oleic acid was deposited by dip-coating using its 10% heptane solution at the withdrawal rate of 1 mm/s. Afterwards the films were dried at 70 °C for 15 min. The samples were irradiated by the same lamps (2 mW/cm^2), the oleic acid degradation being followed by measuring the contact angle for water of the film surface using a Tantec contact angle meter. The decrease in the contact angle for water is expected to depend on the degree of the oleic acid degradation, producing probably more hydrophilic compounds, such as acids with shorter chains, aldehydes, and alcohols. At the final stages of the photocatalytic degradation, the organic layer starts to loose its compactness, which uncovers the hydrophilic TiO_2 surface. In parallel, the change in the mass of the organic layer due to the irradiation was determined.

3. Results and discussion

3.1. Morphological and structural properties of the spray-coated mesoporous TiO_2 films

The variation in the preparation conditions has shown that the concentration of the sol used for spraying is one of the decisive processing parameters. If highly diluted sols (the dilution typically of 1:100) were used, the thickness of the film was in the range of several tens of nanometres only and the films were not sufficiently uniform. If, on the other hand, substantially concentrated sols (above 1:10) were sprayed on the glass slides, the adhesion of the calcined films was not strong enough, which led to an extensive peeling. Therefore, the dilution from 1:10 to 1:20 was found as the best. The width of the sprayed area of 80–100 mm was optimal as spraying on a narrower zone led to too thick layers insufficient in their adhesion, while a layer deposited on a wider area suffered from inhomogeneity. The preheating of the glass support was desirable for two reasons. First it facilitates the evaporation of the solvent present in a large excess, essential for the surfactant enrichment inducing the self-assembly process and the organization into liquid-crystalline mesophases. While the solvent evaporation at ambient temperature was not sufficient to start the self-assembly, a substantially higher temperature of the coated surface prevented the coalescence of particles into a continuous films and led to the formation of individual mesoporous particles and consequently to a powdered material. Second the preheating at 70 °C improved the adhesion of the TiO_2 layers to the glass surface.

Fig. 2 shows SEM images of a typical one-layer film. Even if the pores do not exhibit any long range ordering, in the top view the porosity of the film appears to be homogeneous without any substantial distortions. TEM images, as an example in Fig. 3 shows, prove that titania films are partially crystalline since well resolved (1 0 1) lattice fringes (a distance of 0.35 nm) of TiO_2 anatase nanoparticles can be clearly seen. This conclusion was confirmed by X-ray diffractograms (Fig. 4) exhibiting a strong (1 0 1) reflection at 2θ of ca. 25° due to anatase nanoparticles besides some propor-

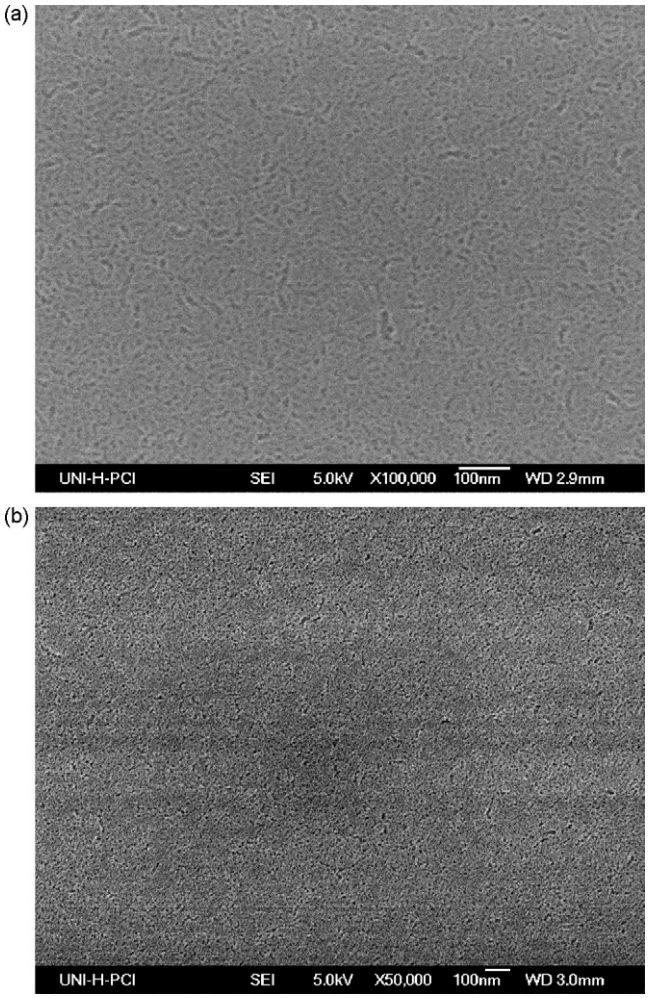

Fig. 2. SEM images of one (a) and two (b) layer films.

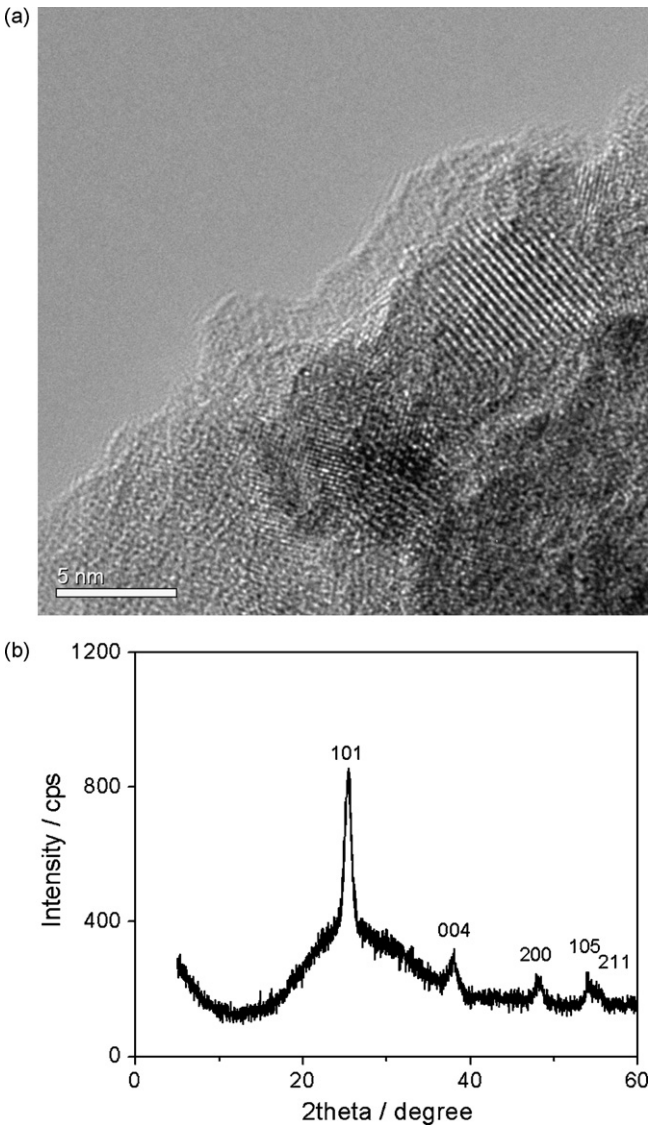

Fig. 3. TEM image (a) and XRD pattern (b) of a one-layer film.

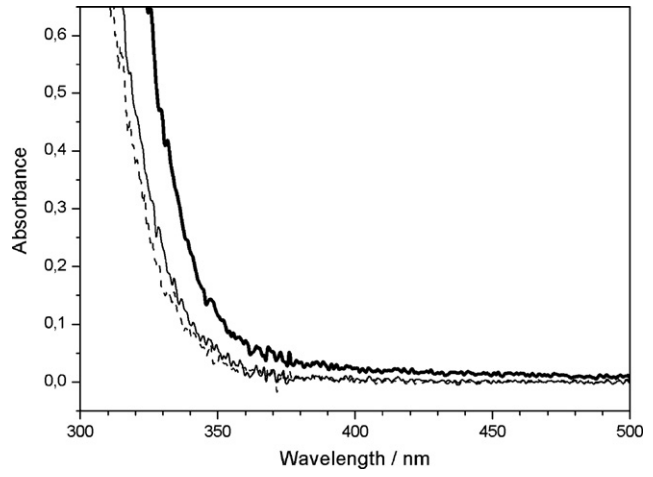

Fig. 4. UV/Vis spectra of one (···), two (–) and three (—) layer films.

tion of amorphous titania leading to the broad background hump at $2\theta = 15–35^\circ$.

A "scotch tape" test showed a good adhesion of the films to the surface of the glass support. Profilometric studies of a number of films provided the thickness of ca. 100 nm per layer. For repeated deposition, the thickness of the films increased approximately linearly with the number of layers.

UV/Vis absorption spectroscopy shows absorption edges for one, two- and three-layer films, respectively (Fig. 4). The small red shift for two- and three-layer films in comparison with the one-layer one is probably due to an increase in the particle size caused by the repeated calcination (twice and three times for the two- and three-layer films, respectively). The repeated calcination of the three-layer film might also lead to some lattice defects, which resulted in the appearance of surface states located within the band gap, explaining the weak absorption at around 400 nm.

From the transmission spectra the optical band gaps E_g can be calculated using the relation

$$\alpha h\nu = A(h\nu - E_g)^n, \quad (1)$$

where α is the absorption coefficient, A is a constant [17]. For the anatase polymorph of TiO_2, the optical transition is indirect, leading to $n = 2$. Furthermore, in the region of strong absorption, and at normal incidence, the reflectivity is very low and can be neglected [18]. This leads to the following expression for the absorption coefficient α as a function of transmittance T

$$\alpha = -2.303 \ \log \frac{T}{t}, \quad (2)$$

where t is the film thickness [18]. Eq. (1) then becomes $-2.303h\nu \log T = B(h\nu - E_g)^2$, and the slope of $(-2.303h\nu \log T)^{1/2}$ versus $h\nu$ provides a linear section that can be extrapolated to zero, leading to E_g. The resulting optical band gaps are $E_g = 3.35$, 3.34 and 3.29 eV for the one-, two- and three-layer films respectively. For all the films the band gap is substantially wider than that of bulk anatase of ca. 3.2 eV, indicating the nanoparticle structure of the pore walls.

In order to determine the texture parameters of thin porous films deposited on supports, whose total surface area is as small as several tens of square centimetres only, a high-sensitive Kr adsorption technique has to be used. The most frequently used adsorptives, namely, nitrogen and argon at ca. 77 and 87 K, respectively, cannot be applied with materials such as thin porous films with very small surface areas. The reason is that the saturation pressures of nitrogen and argon at 77 and 87 K, respectively, are very high, reaching ca. 760 Torr, which leads to an extremely large number of molecules being trapped within the void volume of the sample cell. Because of a very small total pore volume and surface area of such thin porous films, the pressure changes due to the adsorption cannot be measured with a sufficient precision. As an alternative, an adsorptive with a substantially lower saturation vapour pressure should be used, such as krypton at the boiling point of liquid nitrogen, whose saturation pressure equals 1.63 and 2.63 Torr as a solid and a supercooled liquid, respectively.

The information on the pore size and pore volume can be obtained from Kr isotherms by analyzing the shape of their hysteresis loop and the limiting adsorption at saturation pressure as well as by comparison of the adsorption on the samples under study with that on well-defined reference materials. A geometric area of 1 cm^2 of the one-, two- and three-layer films showed specific surface areas of 78, 150 and 222 cm^2, respectively. Clearly the surface area increases practically linearly with the increasing number of coatings, which is in agreement with the linear increase in thickness. Similarly, the specific pore volume (also related to a geometric area of 1 cm^2) calculated from the limiting adsorption increased more or less proportionally with the number of layers, equalling

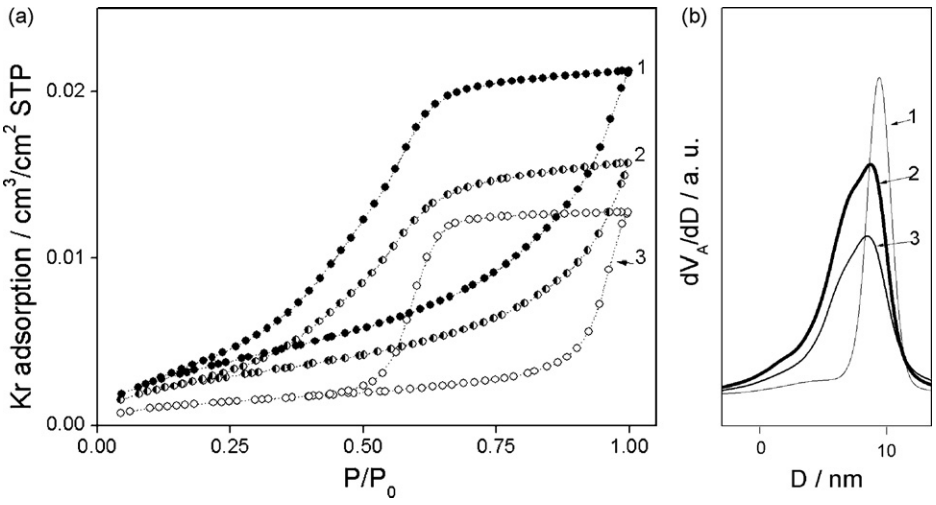

Fig. 5. Adsorption isotherms of Kr at 77 K (a) and corresponding pore size distributions (b) on one (1), two (2) and three (3) layer films.

0.293, 0.359 and 0.483 mm^3/cm^2 for one-, two- and three-layer films, respectively (Fig. 5a).

Other important parameters of porous systems are the mean pore size and the pore size distribution. As the analysis of adsorption isotherms of Kr at 77 K is far from being straightforward and a well-established procedure (e.g. DFT) has not been implemented yet, a simple method based on comparative plots was used [15,16]. As a suitable reference material a non-porous anatase (Aldrich) was used, whose surface area was 11.2 m^2/g. Comparison plots for each sample were constructed, in which the adsorption on the sample under study was plotted against that on the reference material. The differentiation of obtained plots provided an assessment of the pore size distribution for each film (Fig. 5b). There are however two important issues which should be addressed. First it is necessary to scale the *x*-axis of the differentiated comparison plot in the pore size to obtain a true pore size distribution. Second the reliability of the texture data obtained by the analysis of krypton adsorption at 77 K should be carefully assessed. In a recent adsorption study, we prepared a series of mesoporous powders of TiO_2, whose properties were as similar as possible with those of the layers [15,16]. A comparison of the texture properties of powders determined by the theoretical DFT analysis of nitrogen isotherms at 77 K with the krypton data provided a linear correlation between the standard adsorption and the pore size, and proved the closeness of nitrogen and krypton data. In parallel, a study into the texture properties of multilayer film of TiO_2 using the environmental ellipsometric porosimetry showed shown a reasonable agreement with Kr data, which lends an important support to the credibility of the obtained data. Fig. 5b shows that the pore size distribution for the one-layer film is rather narrow, being centred at ca. 10 nm. The two- and three-layer films exhibit wider pore size distributions, which is probably due to the less than perfectly defined way of spray-deposition as well as the repeated calcination. However, the variation in the mean pore size is not substantial, which proves that the procedure developed is suitable for the preparation of films of variable thickness without any substantial change in their porosity.

3.2. Photocatalytic performance of multilayer spray-coated TiO_2 films

During the photocatalytic oxidation, adsorbed NO molecules react first with photogenerated $OH^\bullet$ or $O_2H^\bullet$ radicals to form adsorbed HNO_2, which is subsequently photooxidized to NO_2. NO_2 is either desorbed or further photocatalyticly converted to HNO_3 [5]. The degree of conversion to HNO_3 depends on the residence time of NO_2 in its adsorbed state, which is substantially enhanced by the porosity of the employed photocatalyst [19].

The photocatalytic activity of the investigated samples determined by the NO oxidation can be conveniently expressed as the photonic efficiency ξ, defined as a ratio of the degradation rate of NO to the incident photon flux related to the irradiated area [24]

$$\xi = \frac{hcN_A \Delta \dot{n}_{NO}}{\phi A \lambda}, \quad (3)$$

where h is the Planck's constant, c the light velocity, N_A the Avogadro's constant, $\Delta \dot{n}_{NO}$ the difference between the inlet and outlet flux of NO, Φ the light intensity, A the irradiated area, and λ the wavelength of the UV light. To ensure the comparability of data obtained at different reaction conditions used in this study, the photocatalytic activity of individual samples is given as per cent of the theoretical photonic efficiency equalling the ratio of their photonic efficiency ξ to the theoretic photonic efficiency ξ_{th} corresponding to the complete conversion of the inlet NO stream times 100.

In order to determine how the flow rate of the gaseous mixture through the reactor influences the photocatalytic oxidation of NO on a TiO_2 layer, the linear velocity of the test gas was varied (Table 1). The experiments showed that the per cent of the theoretical photonic efficiency of NO phototransformation was inversely proportional to the linear velocity (Fig. 6). If linear velocity was increased twice from 10 to 20 cm s^{-1} (still corresponding to a laminar flow), the per cent of the theoretical photonic efficiency after switching on the light was decreased by a factor of about 2 from 98 to 48%. Approximately the same ratio still held after 120 min of the experiment when the steady state was achieved. Furthermore, the effect of the distance between the sample and the glass window was determined. An increase in the distance between the sample and the reactor window led to a decrease in the per cent of the theoretical photonic efficiency from 98 to 49% if the distance was increased from 0.4 to 1.0 cm. The irradiation intensity was the same in both cases.

There are two important conclusions to be drawn from these measurements. First, for the practical reasons, especially the limits of the gas flow rate, it is impossible to achieve transition from laminar to turbulent regimes. Second, in spite of the limited mixing due to the laminar regime, practically complete oxidation of inlet NO at the early stages of the experiment was achieved at the linear velocity of 10 cm s^{-1} and the window–sample distance (i.e. the depth of the reactor) of 0.4 cm, corresponding to a space time of ca. 1 s. The observed difference of NO conversion for two different

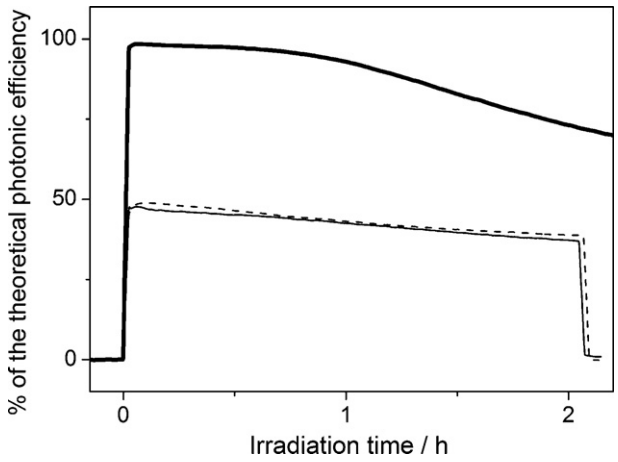

Fig. 6. Effect of the variation in the linear velocity of the gas stream and the distance between the sample and reactor window on the photocatalytic activity. (—) Sample–window distance 0.4 cm, linear velocity 10 cm s^{-1}. (–) Sample–window distance 0.4 cm, linear velocity 20 cm s^{-1}. (···) Sample–window distance 1.0 cm, linear velocity 10 cm s^{-1}.

depths of the photoreactor could be explained by the laminarity of the gas flow.

Fig. 7 shows a long-term time profile of the per cent of the theoretical photonic efficiency of the NO photocatalytic oxidation. Very fast initial increase to almost complete conversion of NO was found immediately after switching-on the light. It was followed by a gradual decrease to a final steady state corresponding to a percent of the theoretical photonic efficiency of ca. 30% being practically independent on the thickness of the film in the range studied. The deactivation observed is likely due to the formation and deposition of nitric acid on the surface. The short-time high photocatalytic activity can be restored by rinsing the photocatalyst with water. The deactivation observed is thus likely due to the formation and deposition of nitric acid on the surface, which is soluble in water and therefore easy to remove by rinsing. The presence of dissolved acid in water used for rinsing was confirmed by a decrease in pH.

The photocatalytic activity of the studied mesoporous films was compared with those of the commercially available self-cleaning glass Pilkington Activ Glass and layers of Degussa P25 TiO_2 prepared by free settling from a water suspension. Neither of the selected reference materials is wholly satisfactory. Generally, it is rather difficult to obtain such reference material, as it should fulfil a number of properties, such as the thickness in the range of several hundreds

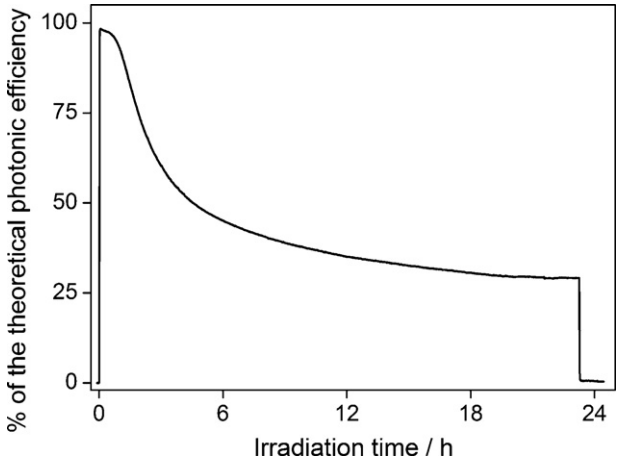

Fig. 7. Photocatalytic oxidation of NO on one-layer film; a long-term experiment. Sample–window distance 0.4 cm, linear velocity 10 cm s^{-1}.

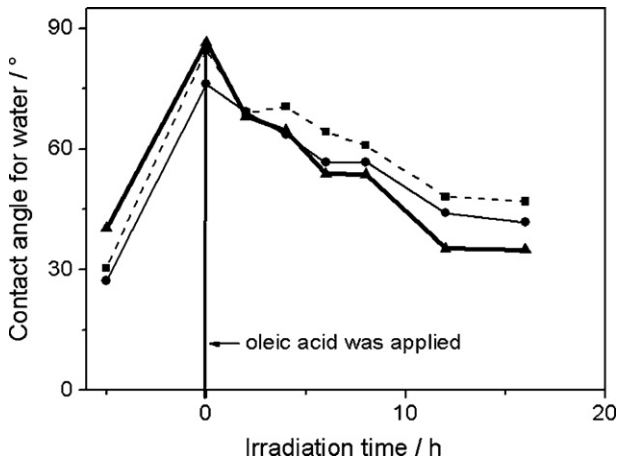

Fig. 8. Photocatalytic decomposition of a thin layer of oleic acid on one-, two- and three-layer TiO_2 films followed by the contact angle measurement.

of nanometers, high mechanical stability, etc. Therefore it would be highly desirable if such a reference material in the form of a layer several hundreds of nanometers in thickness were commercially available. While the activity of the non-porous Pilkington glass was practically negligible, that of the P25 layers was higher (8–10%) but still lower than that of the mesoporous TiO_2 films.

Oleic acid was chosen as a suitable compound to model grease stains on various types of surfaces and their removal by photocatalytic conversion. It is an important industrial and laboratory reagent, and contained in vegetable oils and in the atmospheric aerosol phase. Last but not least, oleic acid was already proposed as a model substance for the ISO test of the self-cleaning ability of surfaces.

Due to the different mechanisms of the photocatalytic oxidation, oleic acid is more appropriate for the mentioned modelling than saturated fatty acids. Generally the reaction of a saturated carboxylic acid with a photogenerated hole leads to a decarboxylation producing the corresponding alkyl radical, as shown for palmitic acid in Ref. [20]. This reaction is favoured by the interaction of the carboxyl group with the TiO_2 surface. Easy addition of dioxygen to the alkyl radical yields an alkylperoxy radical, which can abstract a hydrogen atom from another organic molecule to produce hydroperoxide and a new alkyl radical. Peroxy radicals can also disproportionate under formation of corresponding alcohol and aldehyde/ketone derivatives. According to Ref. [21], in the condensed phase, however, the production of hydroperoxides should predominate over radical recombination.

Unlike saturated fatty acids, oleic acid contains a double bond. In the fist step, the double bond is oxidized to vicinal diols followed by further oxidation to carboxylic groups. Identified primary products of the oxidation are predominantly monocarboxylic nonanoic, 9-oxononanoic and dicarboxylic azelaic acids as well as nonanal [22,23]. Nonanal has a higher vapour pressure and is expected to volatilize. With the increasing oxygen-to-carbon ratio, the droplets containing products of the oleic acid oxidation exhibit higher affinity to water, which facilitates water uptake [22].

Fig. 8a shows an evolution of the contact angle for water during the photocatalytic degradation of oleic acid for one- to three-layer films. The contact angle for water on clean TiO_2 films was around 30°, which is a characteristic value for metal oxide surfaces. After the deposition of a thin layer of oleic acid on the TiO_2 film, the contact angle for water increased to 75–85°. Within 12 h of irradiation, the contact angle for the three-layer film gradually decreased to an original value of the clean film before the deposition of oleic acid. For the one- and two-layer films, the decrease in the contact angle was slower and did not reach the original value within

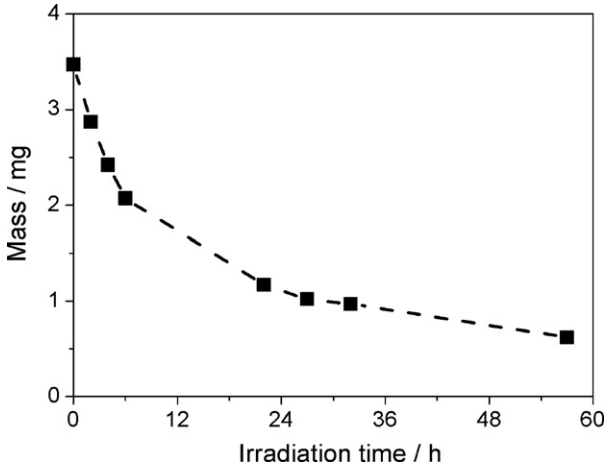

Fig. 9. Decrease in mass of a thin layer of oleic acid deposited on one-layer TiO_2 film during its photocatalytic decomposition.

the 16 h experiment. In Fig. 9, photocatalytic degradation of oleic acid on one-layer film was followed by a gravimetric method. During a 60 h experiment, the mass of the organic layer was gradually decreasing. A major part of the decrease was within the first 20 h that corresponded with the contact angle measurements. We have checked the reproducibility of the photocatalytic performance and found it satisfactorily high.

While the contact angle measurements and the gravimetric method provide valuable information on the oleic acid decomposition, to gain a complete insight into this process the understanding of the mechanism is important. A detailed analysis of the intermediates of the photocatalytic degradation of oleic acid using GC MS is now in progress [25].

4. Conclusions

In summary, mesoporous films of TiO_2 prepared by the low-cost and versatile spraying procedure exhibit a good mechanical properties and a thickness, which can be readily controlled by varying the number of deposited layers, their porosity being homogeneous and their surface area and pore volume increasing practically linearly with the increasing number of deposited layers. They are promising photocatalyst for the photocatalytic oxidation of gaseous pollutants as shown for NO and for the removal of liquid layers of fatty acids deposited on their surface. Therefore they are possible candidates for self-cleaning coatings as they can be easily deposited on objects of various shape and size.

Acknowledgements

The authors are thankful to the Grant Agency of the Czech Republic (grant Nos. 104/08/0435-1 and 203/08/H032), the Ministry of Education, Youth and Sport of the Czech Republic (project 1M0577), and to the German Science Foundation (DFG, grant No. WA 1116/13) for the financial support.

References

[1] J.H. Seinfeld, S.N. Pandis:, Atmospheric Chemistry and Physics: From Air Pollution to Climate Change, Wiley, New York, 1998.
[2] S. Xie, Y. Zhang, L. Qi, X. Tang, Atmos. Environ. 37 (2003) 3213.
[3] M. Luria, R. Weisinger, P. Mordechai, Atmos. Environ. 24B (1990) 93.
[4] S. Vardoulakis, B.E.A. Fisher, N. Gonzalez, Atmos. Environ. 36 (2002) 1025.
[5] S. Devahasdin, C. Fan jr, K. Li, D.H. Chen, J. Photochem. Photobiol. A: Chem. 156 (2003) 161.
[6] F.-L. Toma, S. Guessasma, D. Klein, G. Montavon, G. Bertrand, Ch. Coddet, J. Photochem. Photobiol. A: Chem. 165 (2004) 91.
[7] K. Hashimoto, K. Wasada, N. Toukai, H. Komonami, Y. Kera, J. Photochem. Photobiol. A: Chem. 136 (2000) 103.
[8] F. Bosc, D. Edwards, N. Keller, V. Keller, A. Ayral, Thin Solid Films 495 (2006) 272.
[9] M. Wark, J. Tschirch, O. Bartels, D. Bahnemann, J. Rathouský, Micropor. Mesopor. Mater. 84 (2005) 247.
[10] J. Rathouský, D. Fattakhova-Rohlfing, M. Wark, T. Brezesinski, S. Smarsly, Thin Solid Films 515 (2007) 6541.
[11] J. Tschirch, D. Bahnemann, M. Wark, J. Rathouský, J. Photochem. Photobiol. A: Chem. 194 (2008) 181.
[12] P. Yang, D. Zhao, D.I. Margolese, B.F. Chmelka, G.D. Stucky, Nature 396 (1998) 152.
[13] C.J. Brinker, Y.F. Lu, A. Sellinger, H.Y. Fan, Adv. Mater. 11 (1999) 579.
[14] C. Sanchez, C. Boissiere, D. Grosso, C. Laneerty, L. Nicole, Chem. Mater. 20 (2008) 682.
[15] J. Rathouský, V. Kalousek, Ch. Walsh, A. Bourgeois, Book of Abstracts 5th International Workshop "Characterization of Porous Materials: from Angstroms to Millimeters", New Brunswick, 2009.
[16] J. Rathouský, V. Kalousek, Ch. Walsh, A. Bourgeois, Micropor. Mesopor. Mater. (submitted for publication).
[17] J. Tauc:, Optical Properties of Solids, Academic Press, New York, 1966, pp. 277–313.
[18] A.G. Vedeshwar, J. Phys. III France 5 (1995) 1161.
[19] V. Kalousek, J. Tschirch, D. Bahnemann, J. Rathouský, Superlattices Microstr. 44 (2008) 506.
[20] E. Mularczyk, J. Drzymala, Ind. Eng. Chem. Res. 35 (1996) 788.
[21] V. Romeas, P. Pichat, C. Guillard, T. Chopin, C. Lehaut, New J. Chem. 23 (1999) 365.
[22] H.-M. Hung, P. Ariya, J. Phys. Chem. A 111 (2007) 620.
[23] Y. Katrib, S.T. Martin, H.-M. Hung, Y. Rudich, H. Zhang, J.G. Slowik, P. Davidovits, J.T. Jayne, D.R. Worsnop, J. Phys. Chem. A 108 (2004) 6686.
[24] I. Bannat, K. Wessels, J. Rathouský, T. Oekermann, M. Wark, Chem. Mater. 21 (2009) 1645.
[25] J. Rathouský, V. Kalousek, M. Kolář, J. Jirkovský, Catal. Today (submitted).